EXPERIMENTS WITH AN EXTERNAL JET FLAP

BY

M. J. KRIEGER

PREPARED UNDER CONTRACT

N.o AF 49 (638) - 583

AIR FORCE OFFICE OF SCIENTIFIC RESEARCH

INSTITUTO TECNOLÓGICO DE AERONÁUTICA

São José dos Campos

São Paulo, Brazil

EXPERIMENTS WITH AN EXTERNAL JET FLAP

BY

M. J. KRIEGER

PREPARED UNDER CONTRACT

N.o AF 49 (638) - 583

AIR FORCE OFFICE OF SCIENTIFIC RESEARCH

INSTITUTO TECNOLÓGICO DE AERONÁUTICA

São José dos Campos

São Paulo, Brazil

SUMMARY

The report describes the investigation, in a blower-type wind tunnel, of several external-jet-flap configurations tested between end plates. Comparison is also made with a trailing edge jet flap tested under the same conditions. Tests were made at a Reynolds number of 1.7×10^5 and at jet momentum coefficients up to 2.616, through a range of angles of attack from 0 to 35 degrees.

ACKNOWLEDGMENTS

This research was sponsored by the United States Air Force through the Air Force Office of Scientific Research of the Air Research and Development Command, under Contract No. AF 49 (638)-583.

The author takes pleasure in acknowledging helpful discussions with Professor J.P. Gorecki.

TABLE OF CONTENTS

List of Figures

18 Pressure distribution position 8.

19 Configuration D. Position 2. Variation of lift coefficient and momentum component in lift direction with angle of attack.

20 Variation of total drag and momentum component in drag direction with angle of attack.

21 Variation of aerodynamic characteristics with momentum coefficient and angle of attack.

22 Configuration A. Jet-flap. Variation of lift coefficient with momentum coefficient = 0.

23 Variation of lift coefficient with and C_j.

24 Variation of drag coefficient with and C_j.

25 Variation of aerodynamic characteristics with momentum coefficient and angle of attack.

26 External jet-flap. Variation of lift coefficient with momentum coefficient and angle of attack.

27 Variation of momentum component in lift direction with

28 Variation of total drag and momentum component in drag direction.

29 Comparison of aerodynamic characteristics of the jet-flap and external jet-flap in configuration B, C and D.

List of Symbols

S	Wing area m^2.
C_L	Lift coefficient $\frac{\text{lift}}{qS}$
C_{L_c}	Momentum component in lift direction $\frac{\eta C_j \sin(\alpha+\delta)}{qS}$
C_D	Drag coefficient $\frac{\text{Drag}}{qS}$
C_{D_c}	Momentum component in drag direction $\frac{\eta C_j \cos(\alpha+\delta)}{q}$
$(C_L)_r$	Jet circulation lift coefficient
C_j	Momentum coefficient $\frac{m.v_j}{qS}$
m	Mass flow $\frac{W}{g}$
v_j	Jet velocity based on isentropic expansion $\sqrt{\frac{2k}{k-1} RTG \left[1-\left(\frac{P}{Pn}\right)^{\frac{k-1}{k}}\right]}$ m/sec
p	Free-stream static pressure, kgwt/sq.cm
p_n	Total pressure at nozzle exit, kgwt/sq.cm
q	Free-stream dynamic pressure $\frac{\rho V^2}{2}$ kgwt/sq.m
k	Ratio of specific heats (1.4 for air)
V	Free-stream velocity, m/sec
W	Weight rate of air flow from nozzle, kgwt/sec
α	Angle of attack
δ	Angle of external flap deflection in relation to wing chord.

INTRODUCTION

The purpose of this exploratory work is a comparative experimental study of aerodynamic characteristics of a jet-flap (jet issuing from wing's trailing edge, fig. 1A - Configuration A) with the characteristics of an external jet flap arrangement.

The external-jet-flap consists of a main airfoil and above it an external full-span flap with a slot at its trailing edge through which a jet of compressed air (simulating an engine's exhaust) is ejected.

This arrangement was tested in two configurations.

Configuration B - External-jet-flap above the wing, plain flap at trailing edge retracted, fig. 1B.

Configuration C - External-jet-flap above the wing, plain flap extended, fig. 1C.

The aerodynamic characteristics of configuration C give an indication of performance at take-off while configuration B gives it at cruising speed.

Although not directly related to above-the-wing external-jet-flap configurations, but for the sake of completeness, some experiments were made with the external-jet-flap located at the main airfoil trailing edge, designated configuration D, fig. 1D.

The external-jet-flap system is really a functional integration of propulsion and lift augmentation. Its funda-

mental value is the simplification of engineering problems brought about by the fact that hot exhaust gases are kept away from the main wing structure, simplifying problems of internal ducting and heat insulation.

These advantages can be fully utilized only if the aerodynamic characteristics of the external jet flap are favorable, i.e. thrust is developed efficiently in cruising configurations and lift augmentation is appreciable in take-off or landing configurations.

This report is an exploratory investigation of the aerodynamic characteristics of external-jet-flaps. Tests are comparative only since they were performed at a relatively small Reynolds Number in the free jet of a blower-type wind tunnel.

MODEL AND INSTALLATION

The model of the main airfoil used in these tests had 10 cm chord, 25 cm span and a modified NACA 0021 section, with a thickened trailing edge (T.E. radius = 4 % chord) The external-jet-flap was made of sheet metal. Its shape and dimensions are shown in fig. 3. The slot along the trailing edge through which the jet issued was 0.25 $\pm$ 0.02 mm wide.

Both the main airfoil and the external-jet-flap were assembled between two rectangular end plates. The central parts of both end plates are discs which can rotate. In

each disc there is a radial slot where the ends of the external-jet-flap are attached. This setup allows the external-jet-flap to be located in any desired position in relation to the main airfoil. Furthermore this setup allows changing of the angle of attack while conserving the established relative position of the main airfoil and external-jet-flap.

Compressed air for the external-jet-flap (configurations B,C,D) or for the plain-jet-flap (configuration A) was supplied from both sides through flexible tubes of 4.8 mm ID.

The airfoil and end-plate assembly was suspended through thin wires on a three component balance, and placed in the free jet, 20 x 30 cm, of a blower type wind-tunnel (fig. 4 and 5).

The weight rate of air flow through the TE slot was determined by means of a calibrated nozzle. Temperature and pressure for determining jet exit velocities were measured at points indicated on fig. 4.

For pressure distribution tests, the model of the main airfoil was fitted with a single chordwise row of pressure taps at midspan, located as shown on fig. 2. Tubes leading from these pressure taps were brought out through both ends of the model and connected to a multiple manometer.

TESTS

Tests were carried out on configurations B, C, D and on a jet-flap model (jet at trailing edge deflected 60 degrees) - configuration A, through the range of angle of attack from zero to 35 degrees.

All the tests were made in the free jet of a blower type wind-tunnel. Average dynamic pressure was 27.0 kgwt/m^2 corresponding to a velocity of 21.8 m/sec. The average test Reynolds number was 1.7×10^5.

The test results are given without correction for wind-tunnel boundary effects, except for the tare drag of the end plates, wire suspension and compressed air connections to the model.

The aerodynamic characteristics of the trailing edge jet-flap were adopted as a standard of comparison for test data on external-jet-flap configurations. For this reason quantitative test data should be regarded only as a means of comparing relative merits of configurations tested. See ref. 1 and 2 for jet flap data obtained in a standard wind tunnel and corrected for tunnel boundary effects.

In all tests the momentum coefficient was based on the main airfoil area. The theoretical jet velocity was calculated assuming isentropic expansion to free stream static pressure. The nozzle efficiency can be obtained from fig.16 which presents variation of measured thrust and lift com-

ponents with momentum coefficient under conditions of zero external flow.

To determine the most favorable location for the external-jet-flap the investigations were carried out in positions shown in fig. 6. For configuration B, the jet-flap was tested in 29 positions. For configuration D, in 8 positions, and finally for configuration C in 12 positions.

In each position preliminary force tests were made to determine maximum lift and corresponding drag. All these tests were made at constant momentum coefficient $C_j = 0.602$.

In configuration B, position 22 was chosen as the best location of an external jet flap of the size and section tested. In configuration C the best location was position 8.

It so happens that position 22 and position 8 are very near to each other. The choice was made on the basis of maximum lift coefficient, disregarding values of drag.

It was found experimentally that maximum lift depended on the angle of inclination of the external-jet-flap in relation to the main airfoil chord. Experiments showed that maximum lift in configuration B occured at $\delta = 5$ degrees. Tests were made for $\delta = 0, 5$ and 10 degrees but not at intermediate values. In configuration C the maximum lift occurred at $\delta = 0$.

An investigation of pressure distributions has been carried out on the same model in configurations B and C. Tests were made at the same average dynamic pressure q = 27

kgwt/m^2 at α = 0, 10, 20 and 30 degrees with momentum coefficient c_j = 0.602, 1.621 and 2.616. The pressure distribution, due to the flow entrained by the jet alone, was also recorded at zero forward speed for each configuration.

After test conditions were stabilized, multiple manometer indications were recorded photographically in all these cases.

DISCUSSION OF RESULTS

The jet sheet ejected chordwise above the upper wing surface over the whole wing span acts in a similar way to a trailing edge jet flap. The lift of such a wing consists of the basic lift of the airfoil due to the angle of attack, momentum lift due to the vertical component of jet reaction and an incremental lift due to increased circulation induced by the jet sheet.

$$C_L = (C_L)_{c_j=0} + C_j \sin(\alpha+\delta) + (C_L)_r$$

For each configuration tested the total lift was broken down into these components. The variation of jet circulation lift coefficient is shown in figure 11 and 15. For configuration B (plain flap up) this coefficient is increasing with momentum coefficient. Up to α = 15 degrees the increase is slow with the angle of attack; above that the increase is rapid and at 30 degrees its value is nearly the

same and independent of the amount of blowing, above C_j = 0.602. This picture is reversed for configuration C (plain flap down). Here the value of the jet-circulation lift coefficient is decreasing with the increased momentum coefficient. This reversed condition was obviously caused by the large deflection (60 degrees) of the plain flap.

Performance of this configuration could probably be improved by correlating the plain flap deflection, external flap location and amount of blowing.

In all configurations mutual interference of wing and external flap without blowing was negative. From tests, the value of maximum lift coefficient of the main airfoil was 0.79, that of external flap alone based upon main airfoil area was 0.231, while total C_L max of this configuration was 0.474. The situation is changed, however, by the action of the jet. Blowing at the momentum coefficient c_j = 1.621, C_L max. is 2.007, the momentum reaction in the lift direction was 0.647 which gives an increase due to jet circulation $(C_L)_r$ = 0.883. The lift produced by the effect of the jet is about three times as large as that due to the jet reaction alone.

For higher values of momentum coefficient the stall does not occur even at high angles of attack. The mechanism of flow reattachment could be explained by the action of a tangential jet of high velocity which energises the boundary layer along the rear upper wing surface, fig. 17 and 18. (Pressure distribution).

The test positions chosen in both configurations were optimized for maximum lift coefficient but not for minimum drag. The total drag values for these configurations are presented in fig. 9 and 14. The same diagrams show also the components which affect total drag, that is, jet-off drag and jet momentum components in the drag direction. The test results on the drag for the trailing edge jet flap are given in fig. 24 and 29. In configuration B, the drag is already negative (thrust) for momentum coefficients above approx. 0.4 ; in configuration C the drag becomes negative above $C_j = 1.1$.

It is believed that with smaller deflection angles of the plain flap, not only will the drag be smaller, but also as previously mentioned, lift might increase due to a possible change of jet circulation.

CONCLUSIONS

The external jet-flap arrangement produced jet induced circulation which warrants further study. The results indicated in fig. 29 show considerable lift augmentation - not as large as a trailing edge jet-flap (60 degrees), but with considerably larger thrust in both configurations.

On the basis of these results it appears that external jet-flap arrangements could be applied to STOL aircraft.

To shorten ground-run at take-off the higher thrust

produced in configuration B (plain flap up) could be utilized to accelerate the aircraft to unstick velocity, then changing to configuration C (plain flap deflected) would produce a higher lift coefficient and still enough thrust to accelerate during transition and climb.

It is believed that aerodynamic characteristics of the configurations tested could be better with a larger scale model. Since the entrainment of air by a jet is essentially a viscous effect, sensitive to turbulence, a larger scale model is necessary to optimize the design of external jet flaps.

REFERENCES

1. Lockwood, V.E., Turner, T.R. & Riebe, J.M. -
Wind-tunnel investigation of jet-augmented flaps on a rectangular wing to high momentum coefficient.
NACA Technical Note 3865

2. Lowry, J.G. & Vogler, R.D. -
Wind-tunnel investigation at low speeds to determine the effect of aspect ratio and end plates on a rectangular wing with jet flaps deflected 85°.
NACA Technical Note 3863.

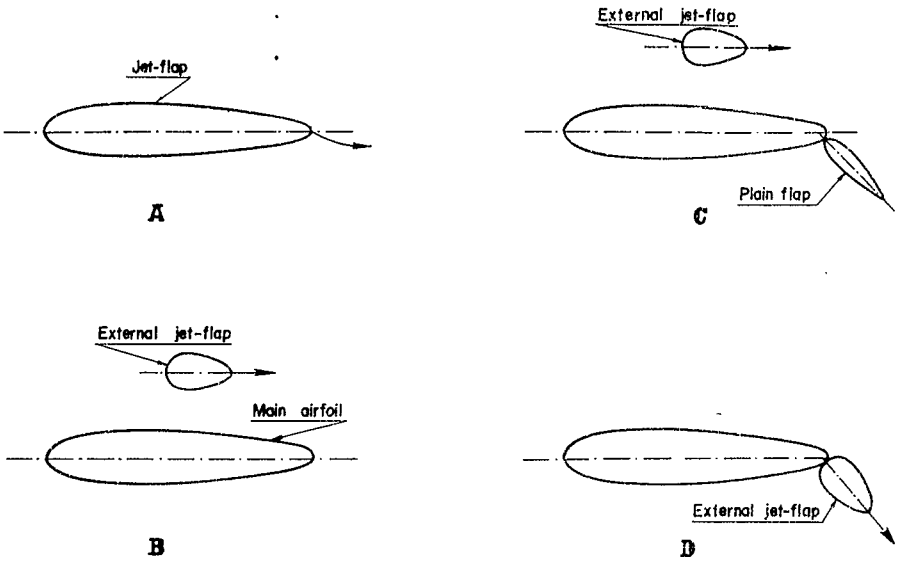

Fig. 1- Tested configurations

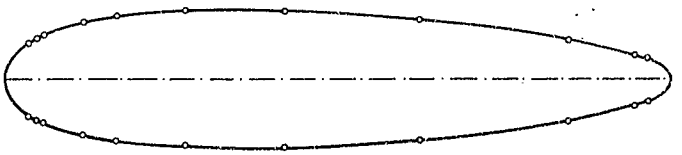

Fig. 2 - Location of pressure orifices

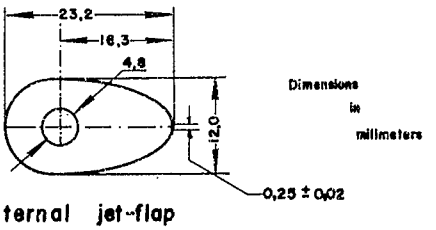

Fig. 3 - External jet-flap

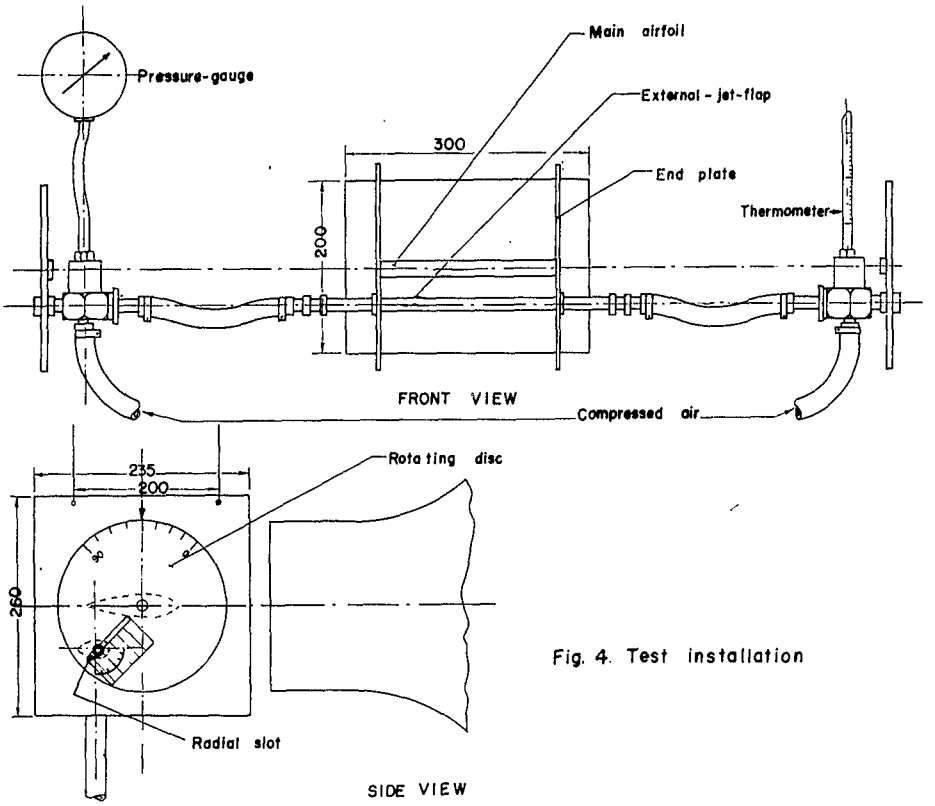

Fig. 4. Test installation

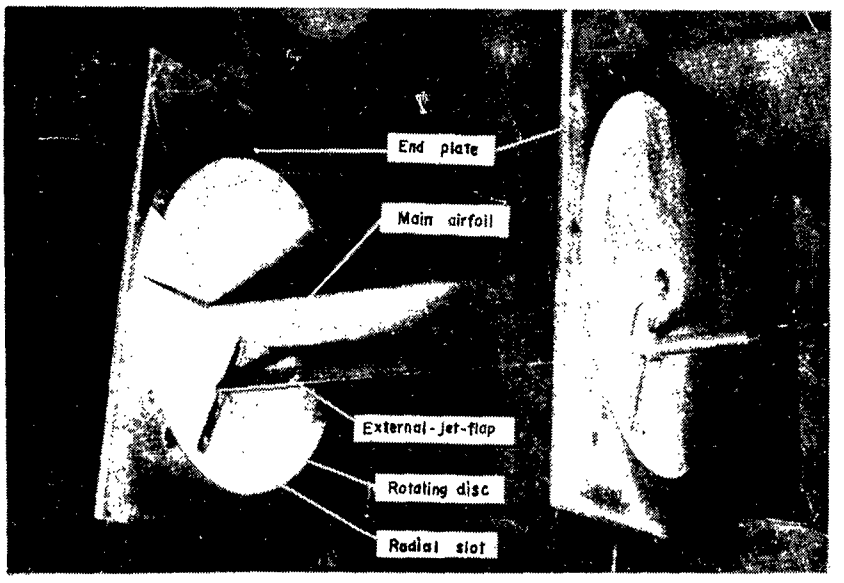

Fig. 5. View of test installation

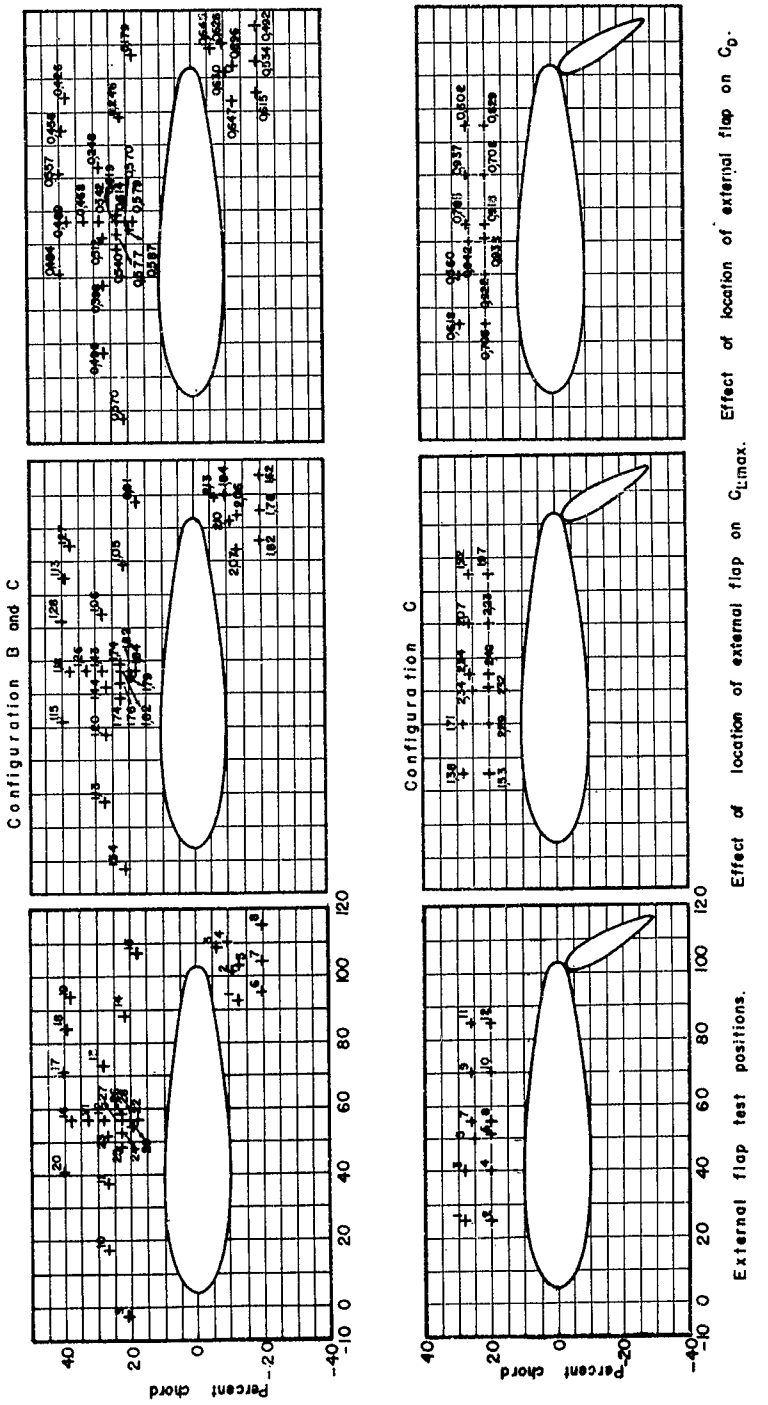

External flap test positions. Effect of location of external flap on $C_{L\,max.}$ Effect of location of external flap on C_D.

Fig. 6 External jet-flap test positions

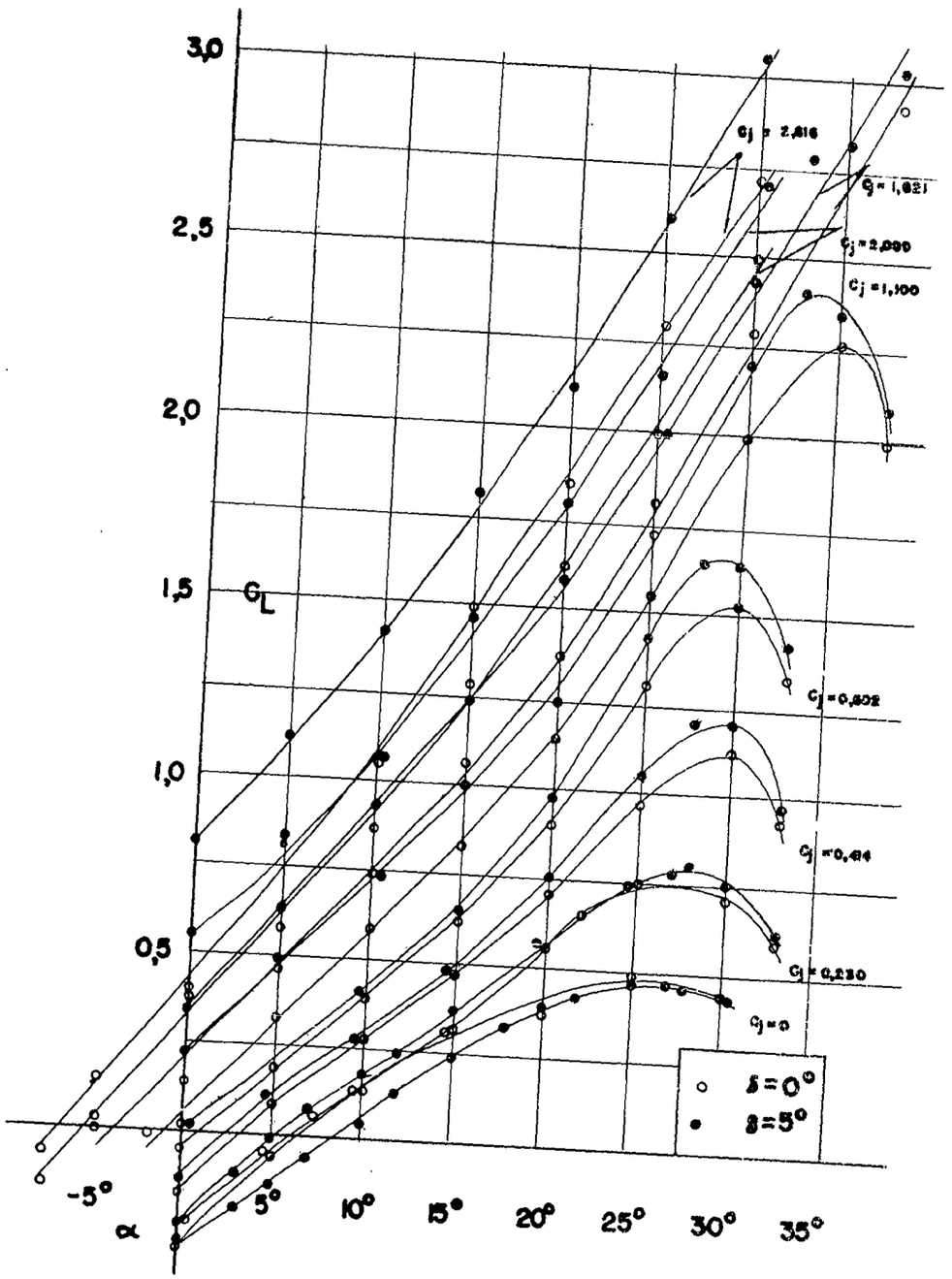

Fig. 7 POSITION 22 — Variation of lift coefficient with momentum coefficient C_j and α

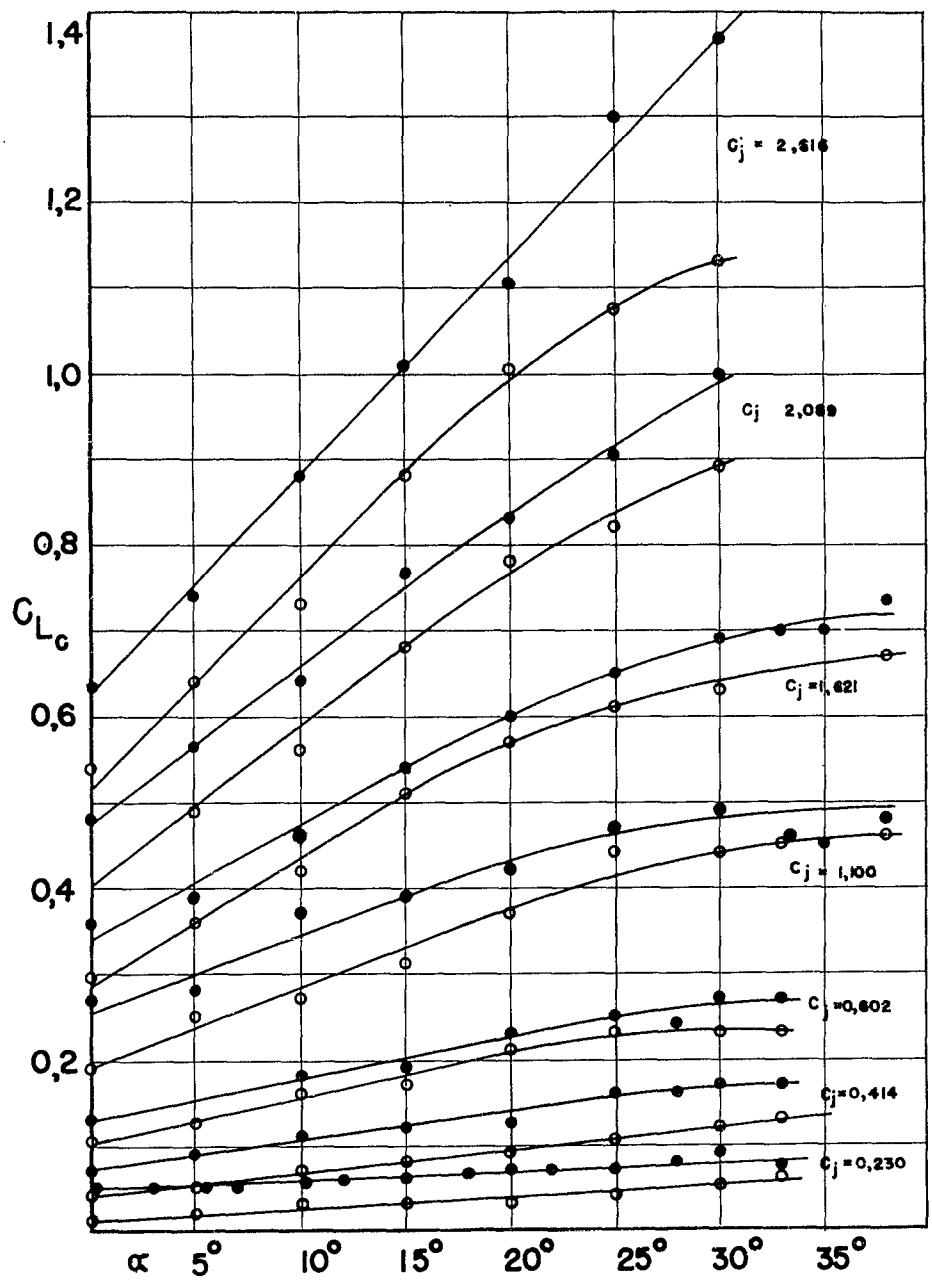

Fig. 8. POSITION 22-Variation of momentum component in lift directions with angle of attack. ○ δ=0 —— ● δ = 5°

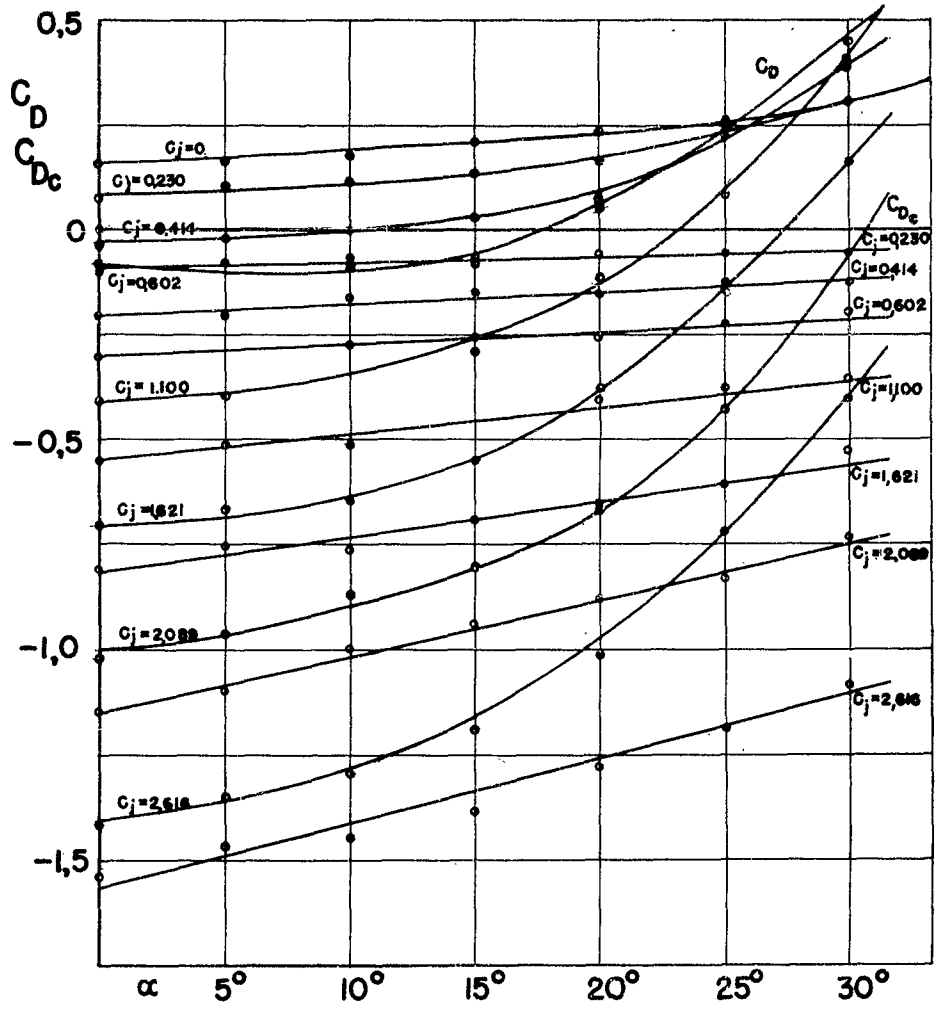

Fig. 9. POSITION 22 — Variation of total drag coefficient and momentum component in drag direction with α $\delta = 5°$.

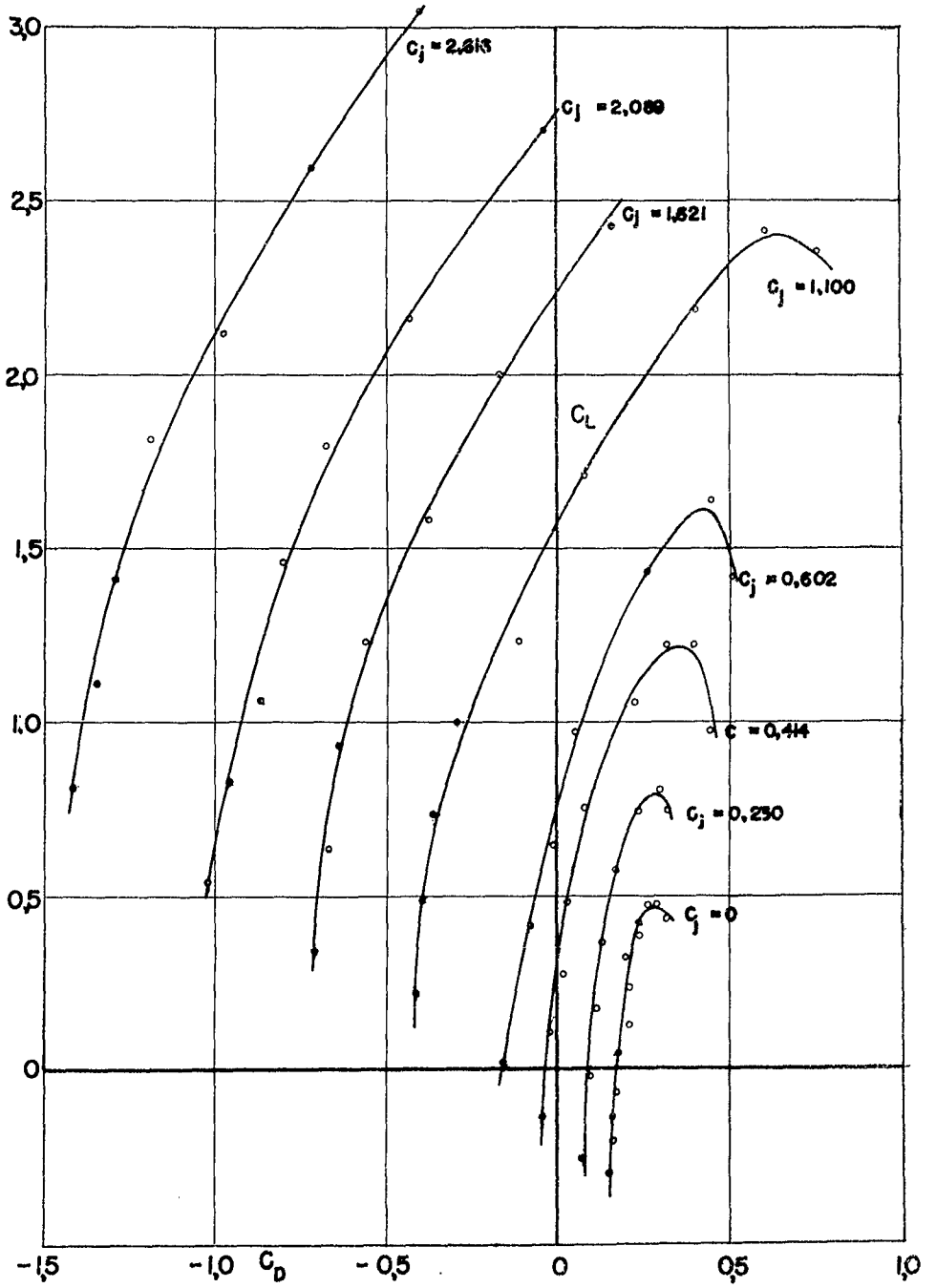

Fig.10. POSITION 22.6 = 5° — Variation of aerodynamic characteristics with C_j and α

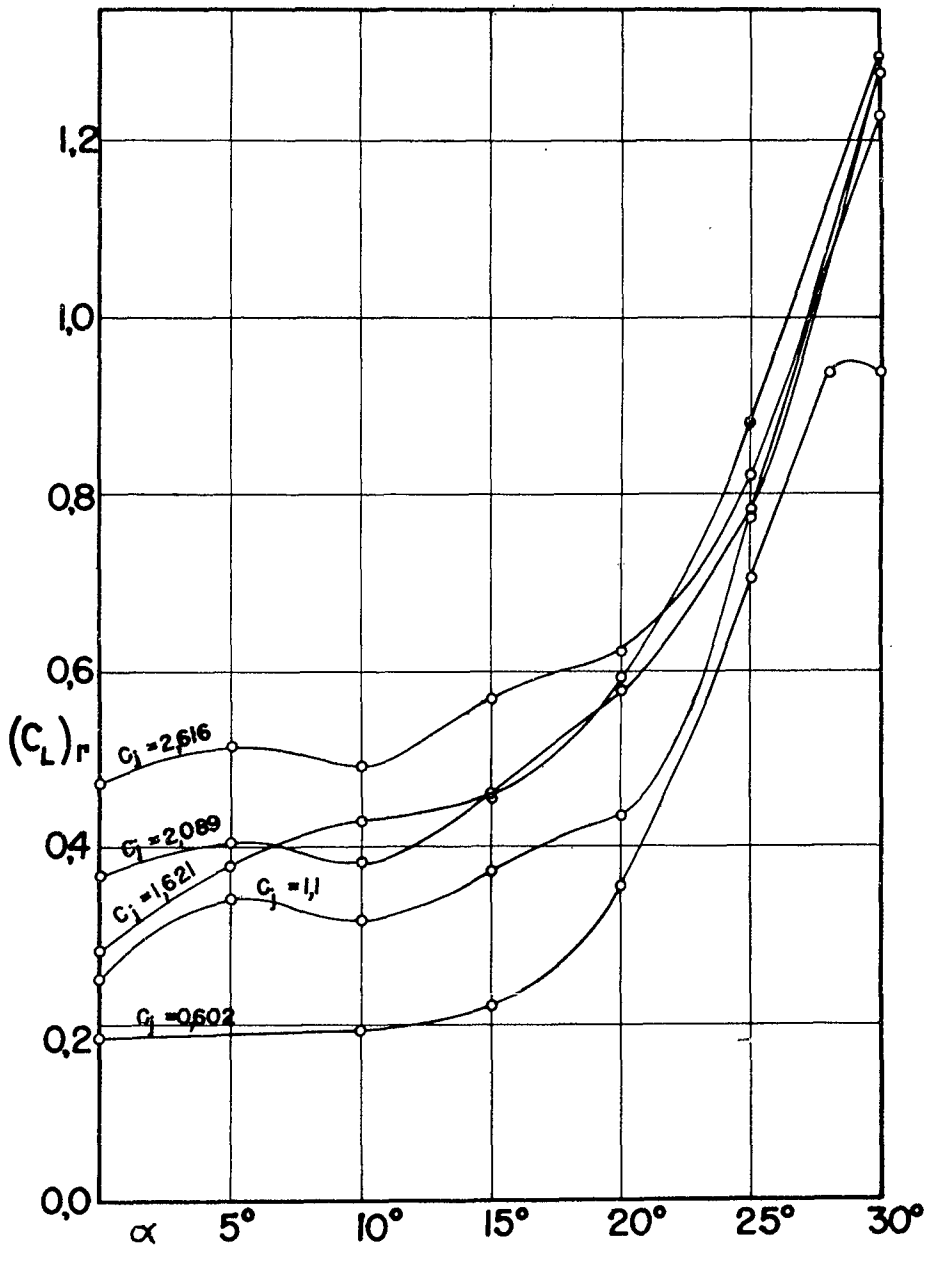

Fig-11. POSITION 22- Variation of jet-circulation lift coeff. with angle of attack and momentum coefficient.

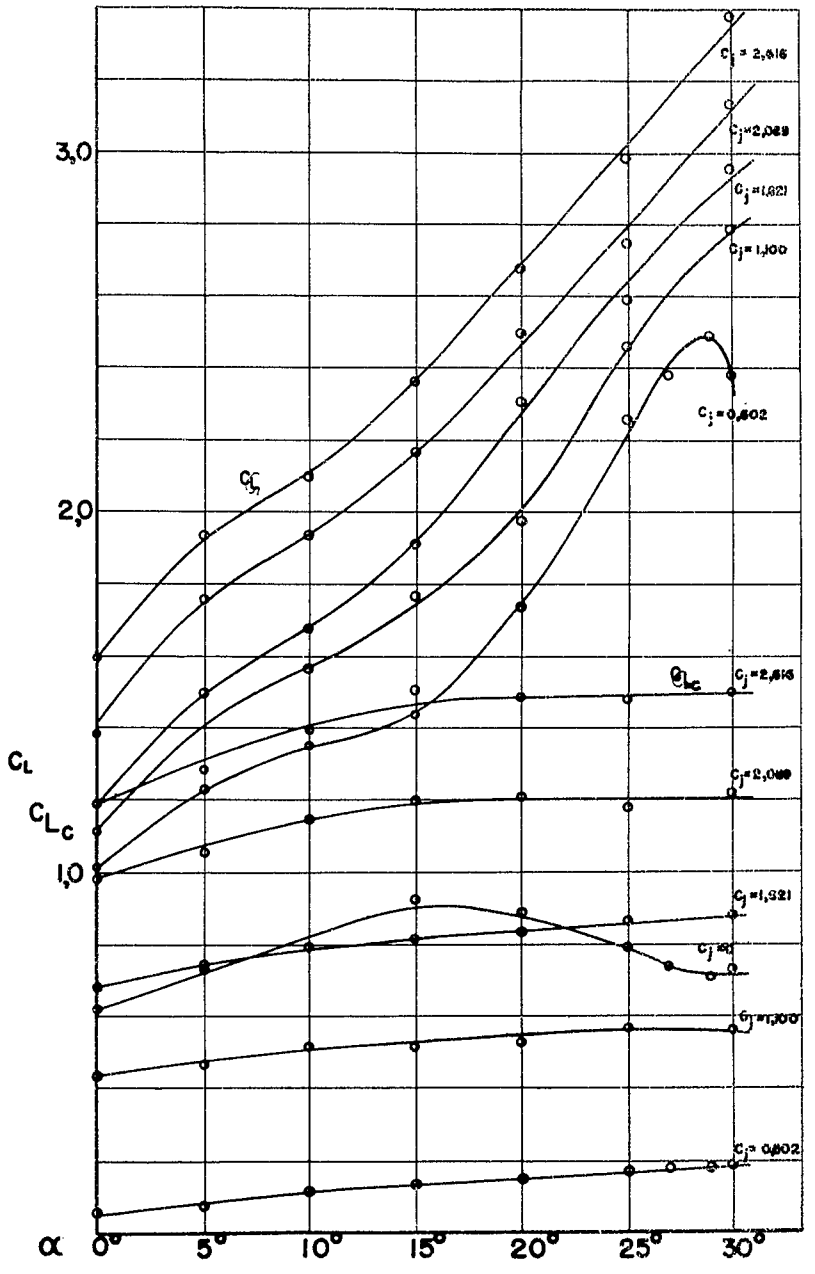

Fig.12. POSITION 8 — Variation of lift coefficient and momentum component in lift direction with C_j and α.

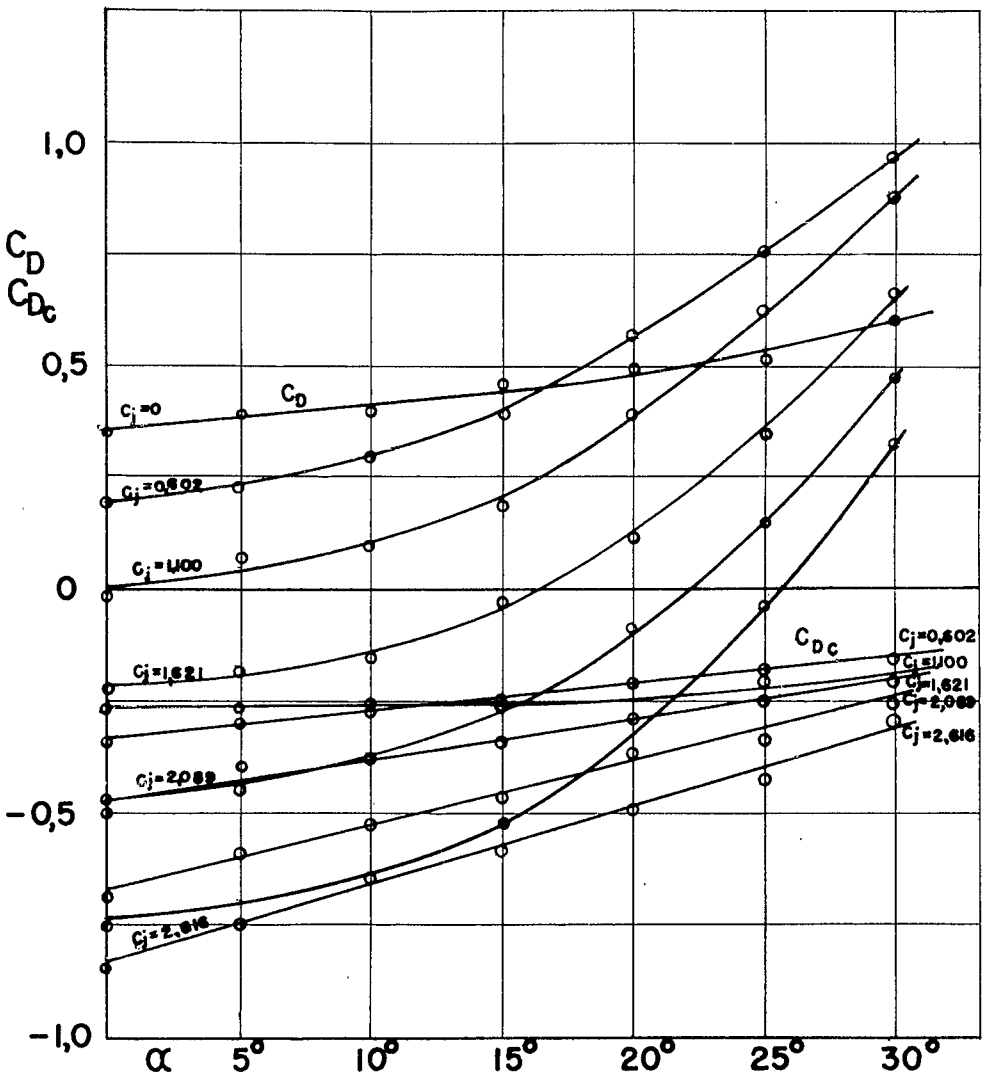

Fig.13. POSITION 8— Variation of total drag coefficient and momentum component in drag direction with α.

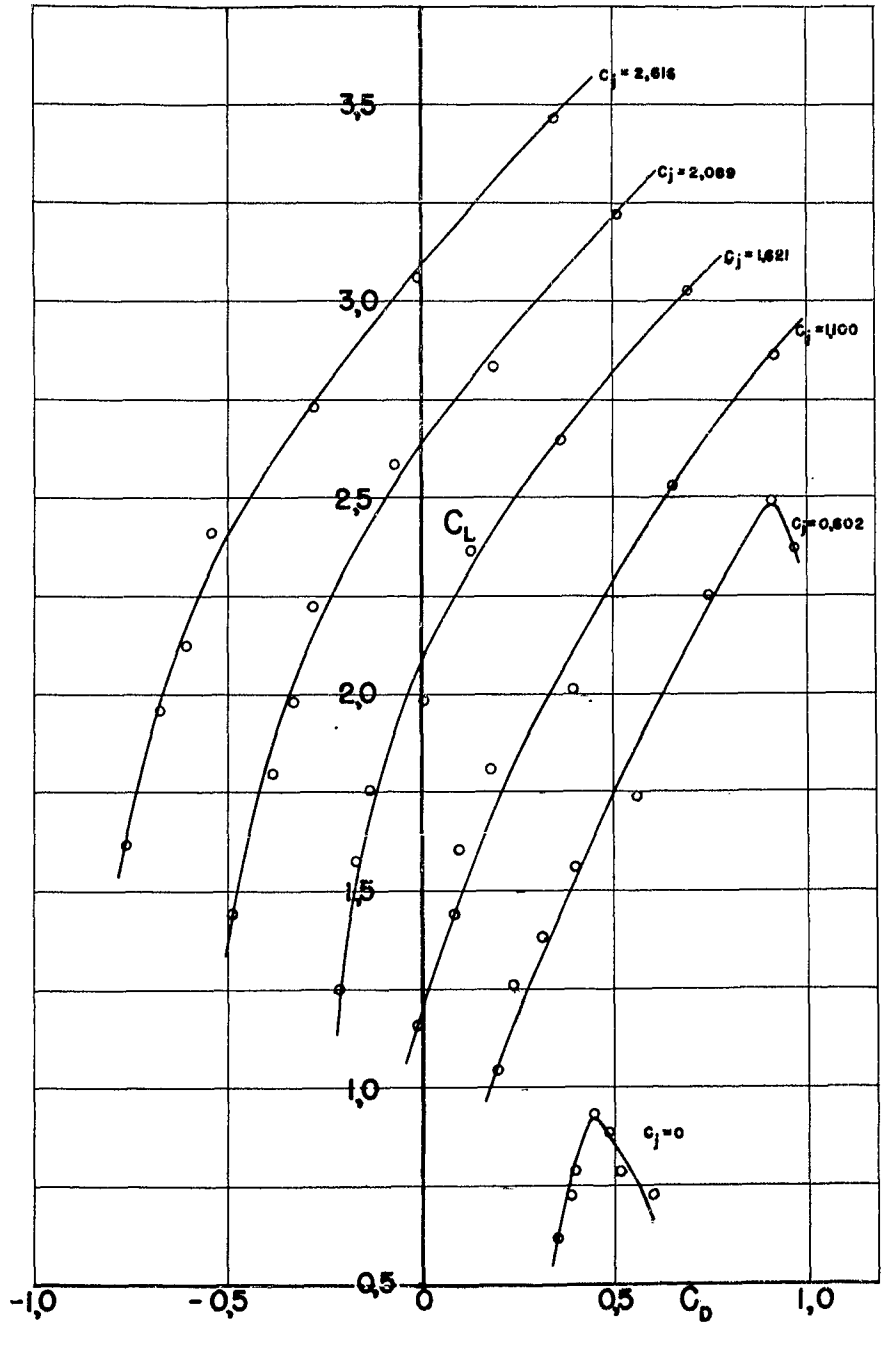

Fig. 14. POSITION 8 — Variation of aerodynamic characteristics with C_j and α - $\delta = 0$

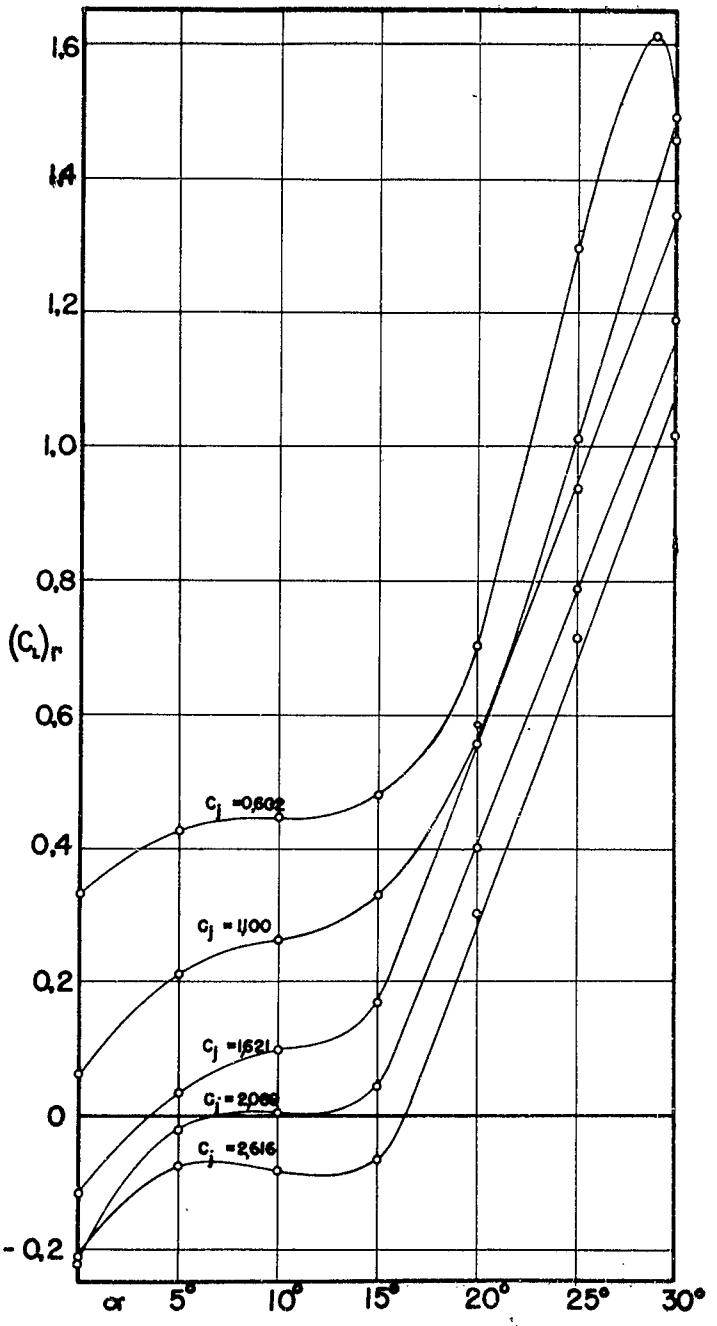

Fig. 15. POSITION 8 — Variation of jet circulation lift coeff. with angle of attack and momentum coefficient..

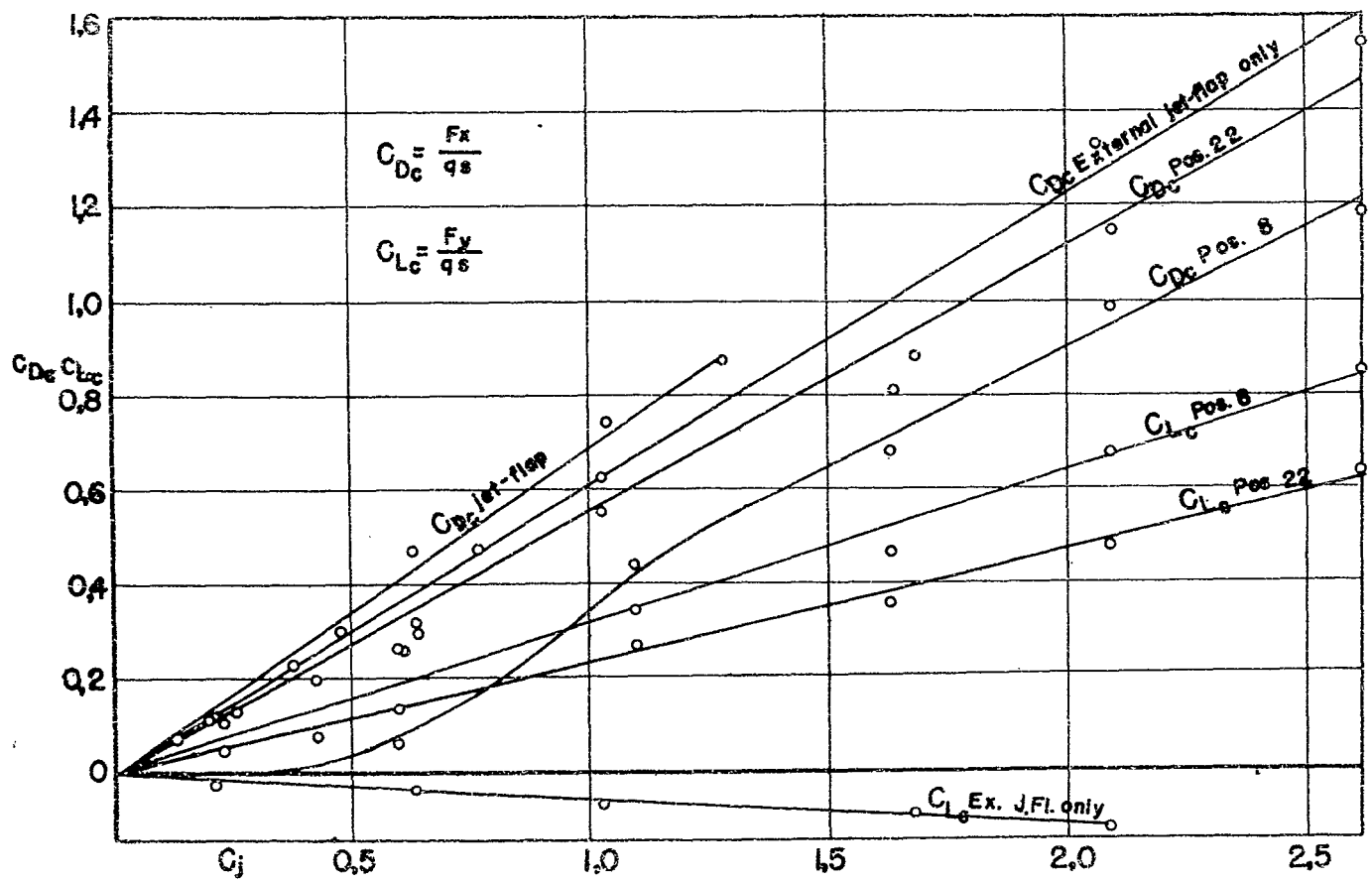

Fig. 15 Variation of measured vertical and horizontal components of thrust coefficient $\alpha=0$ $q=0$ $\delta=0$

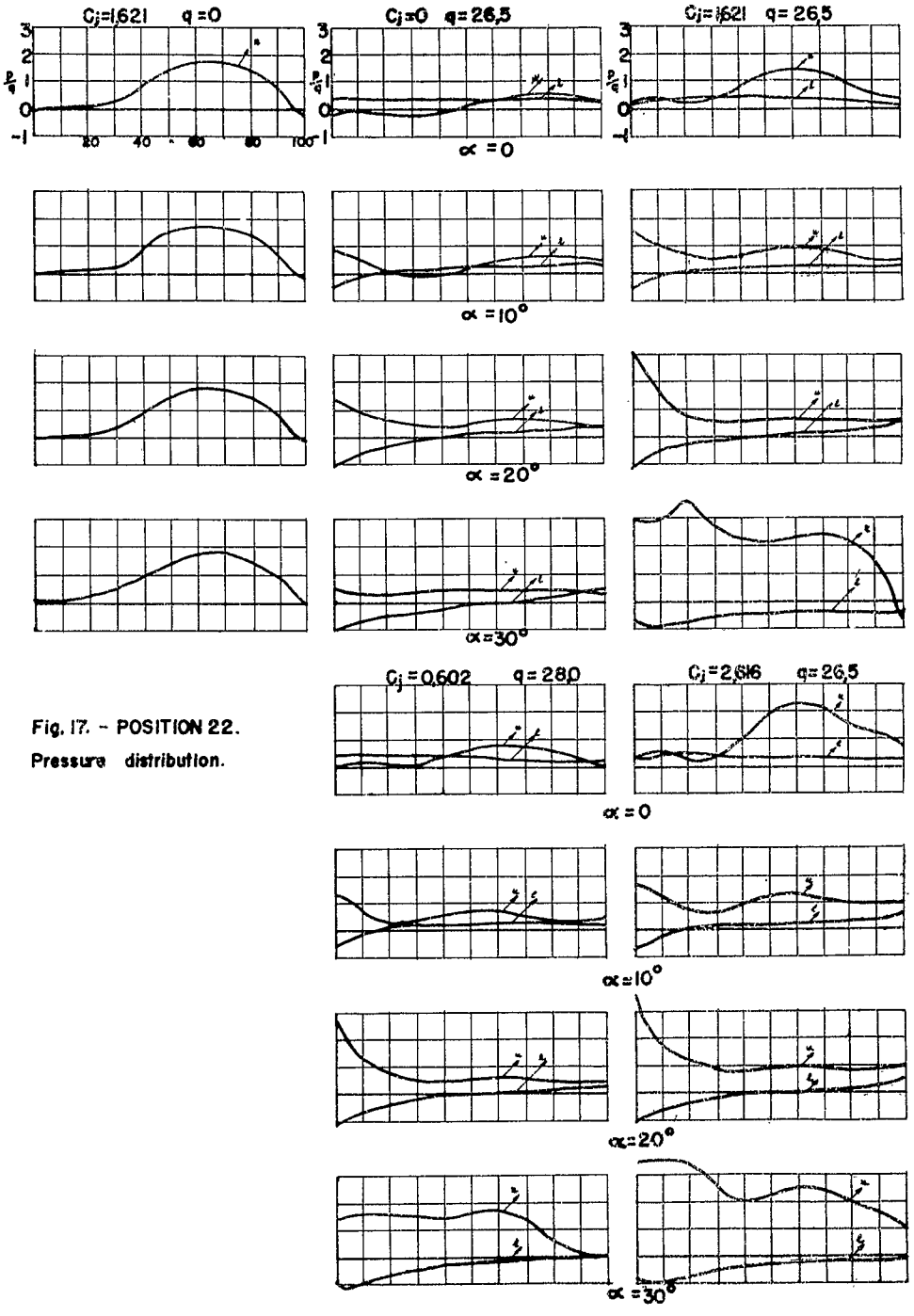

Fig. 17. – POSITION 22.
Pressure distribution.

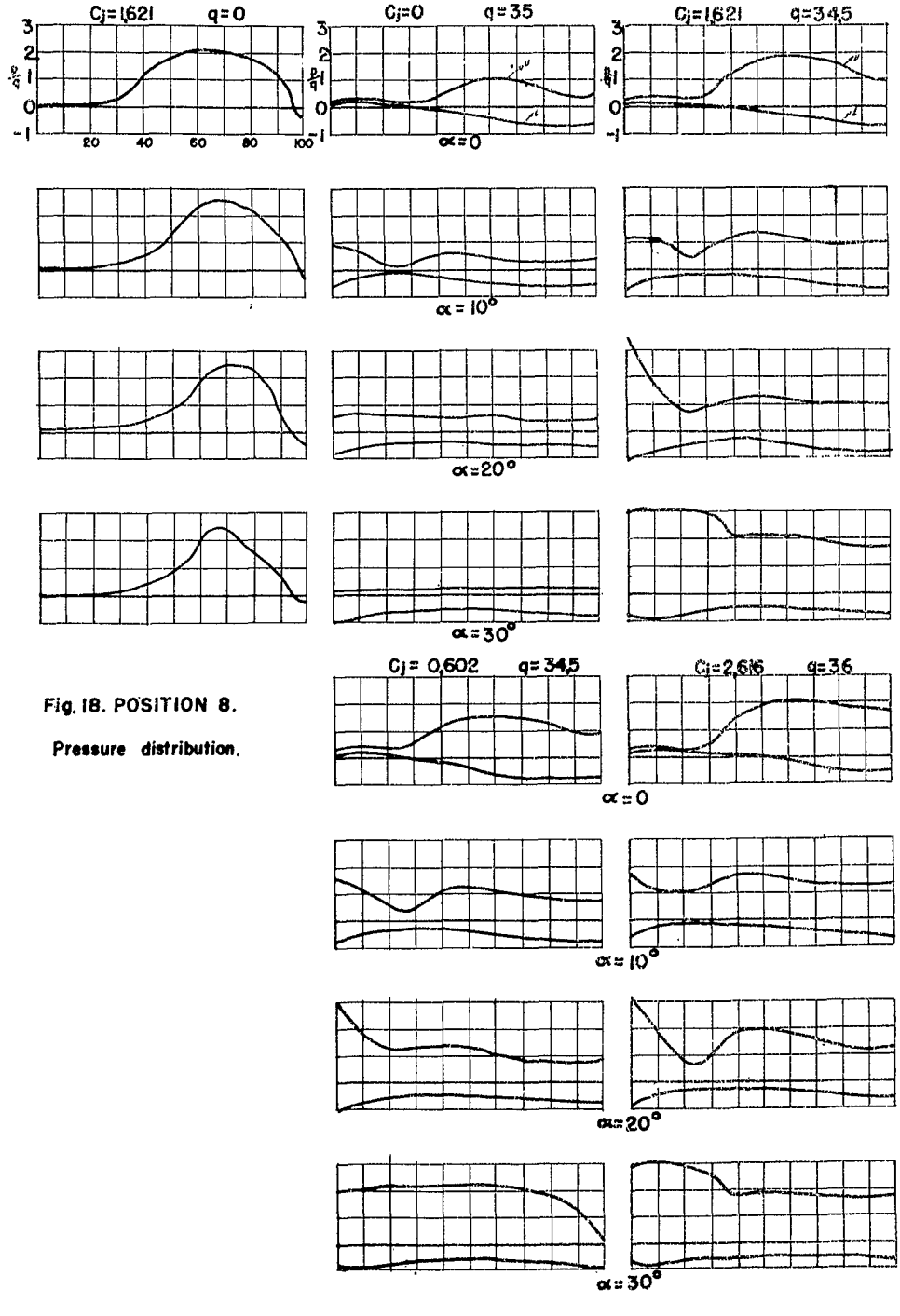

Fig. 18. POSITION 8.

Pressure distribution.

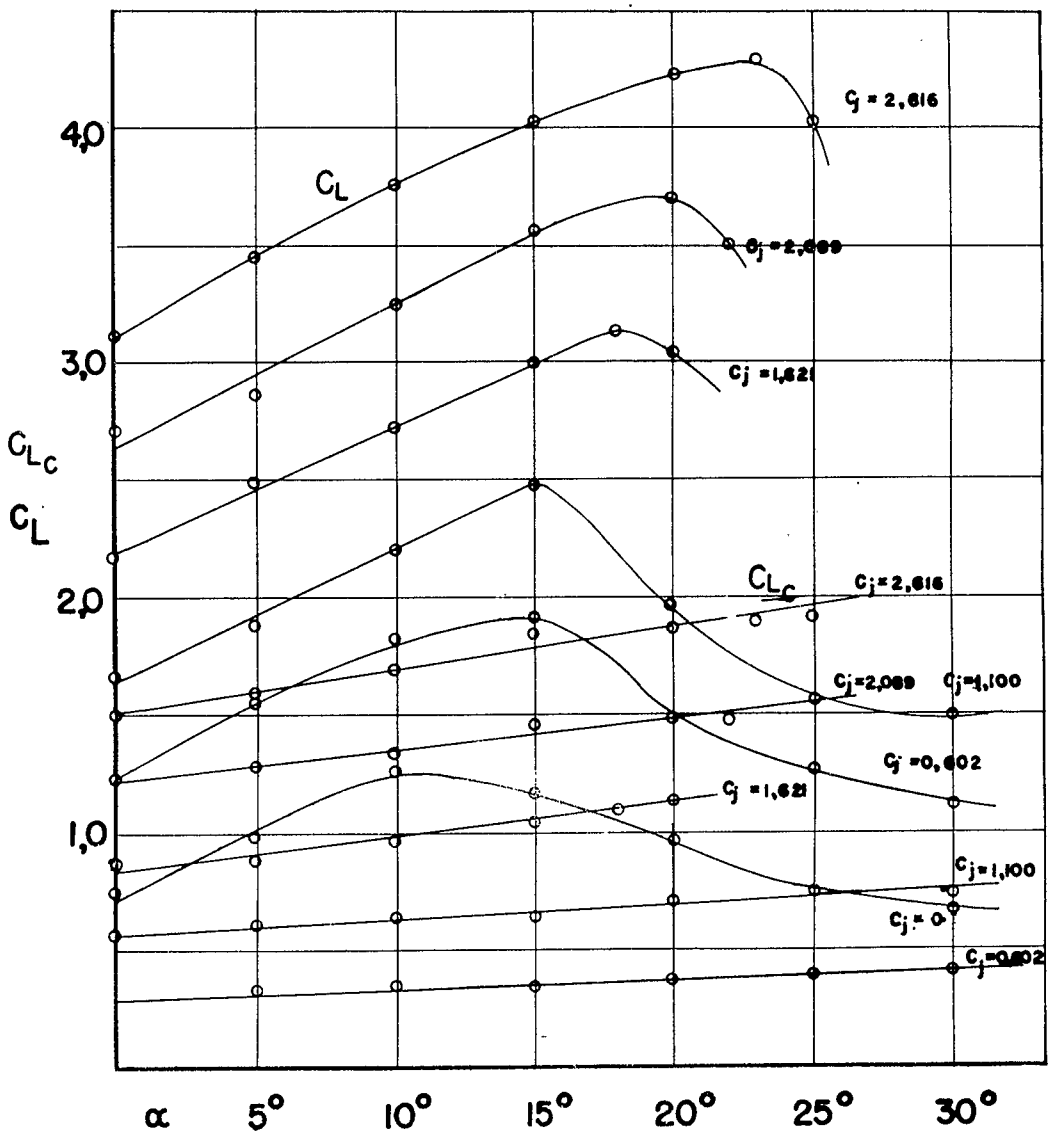

Fig. 19. POSITION 2 — Variation of lift coefficient and momentum component in lift direction with C_j and α

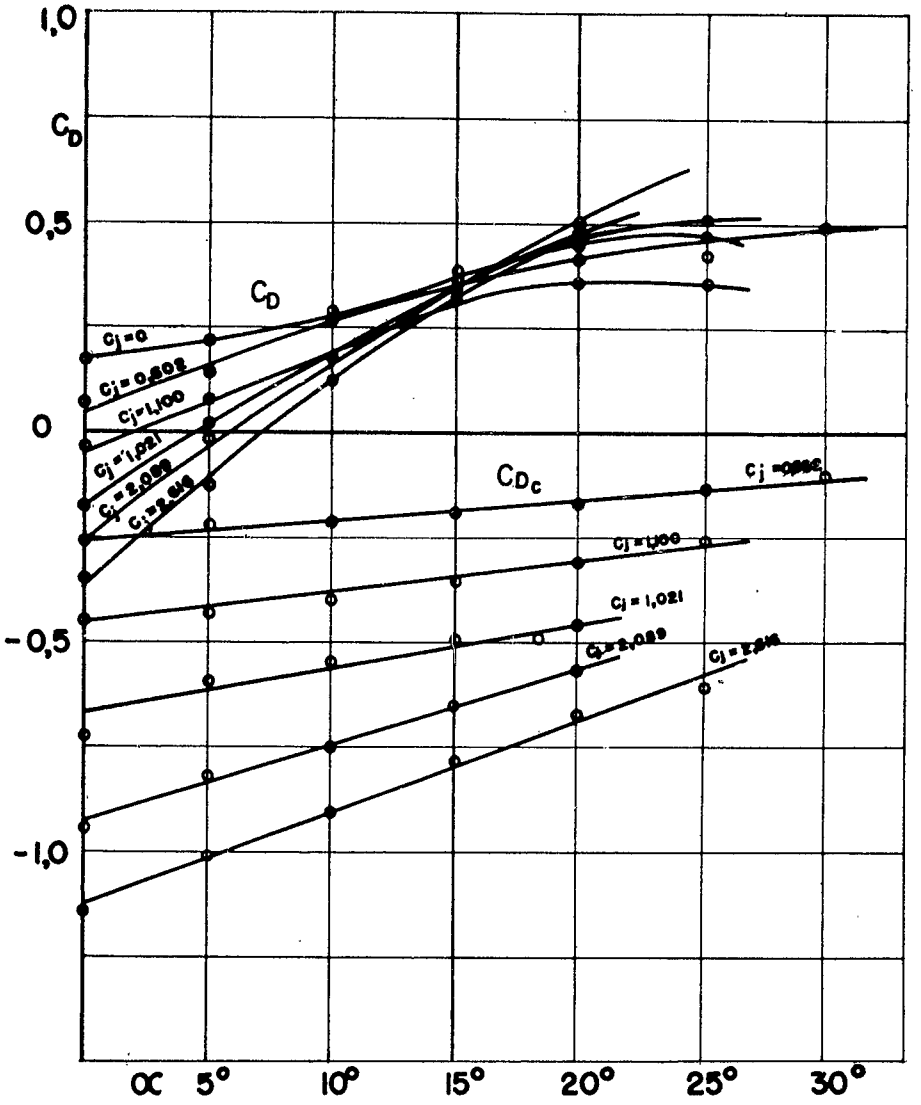

Fig. 20. POSITION 2 – Variation of total drag coefficient and momentum component in drag direction with α and C_j

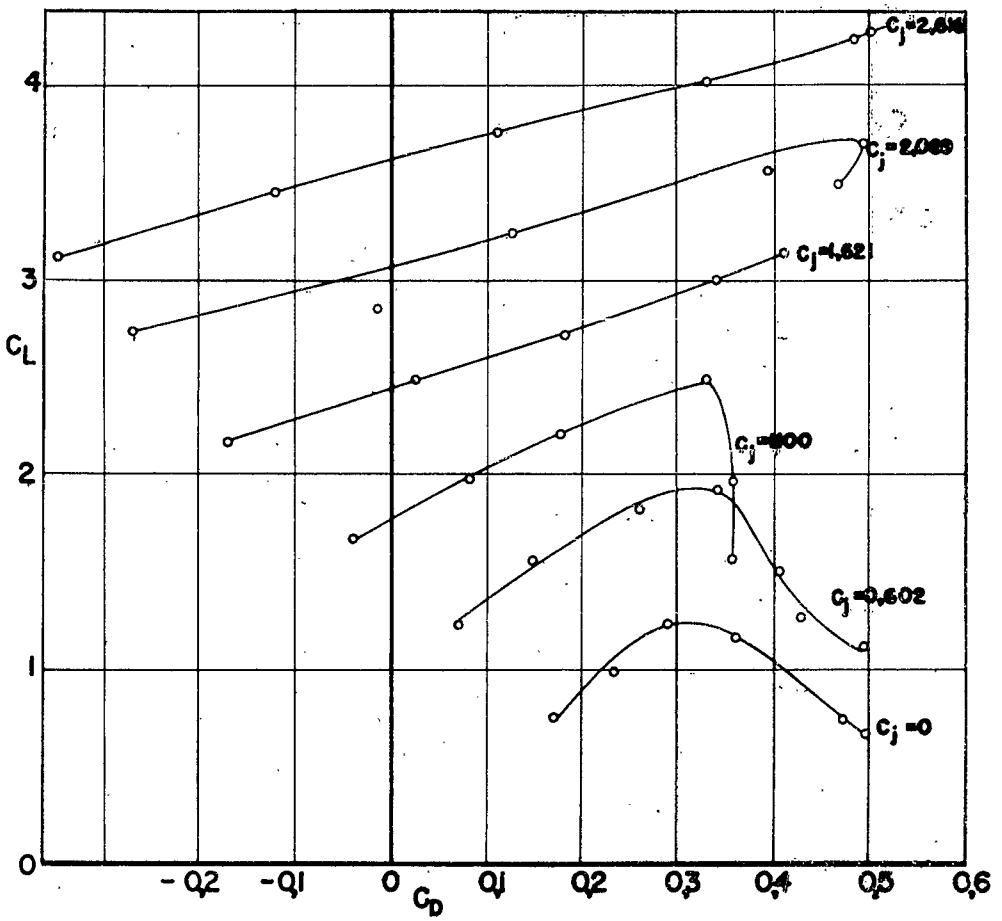

Fig. 21. POSITION 2 – Variation of aerodynamic characteristics with C_j and α.

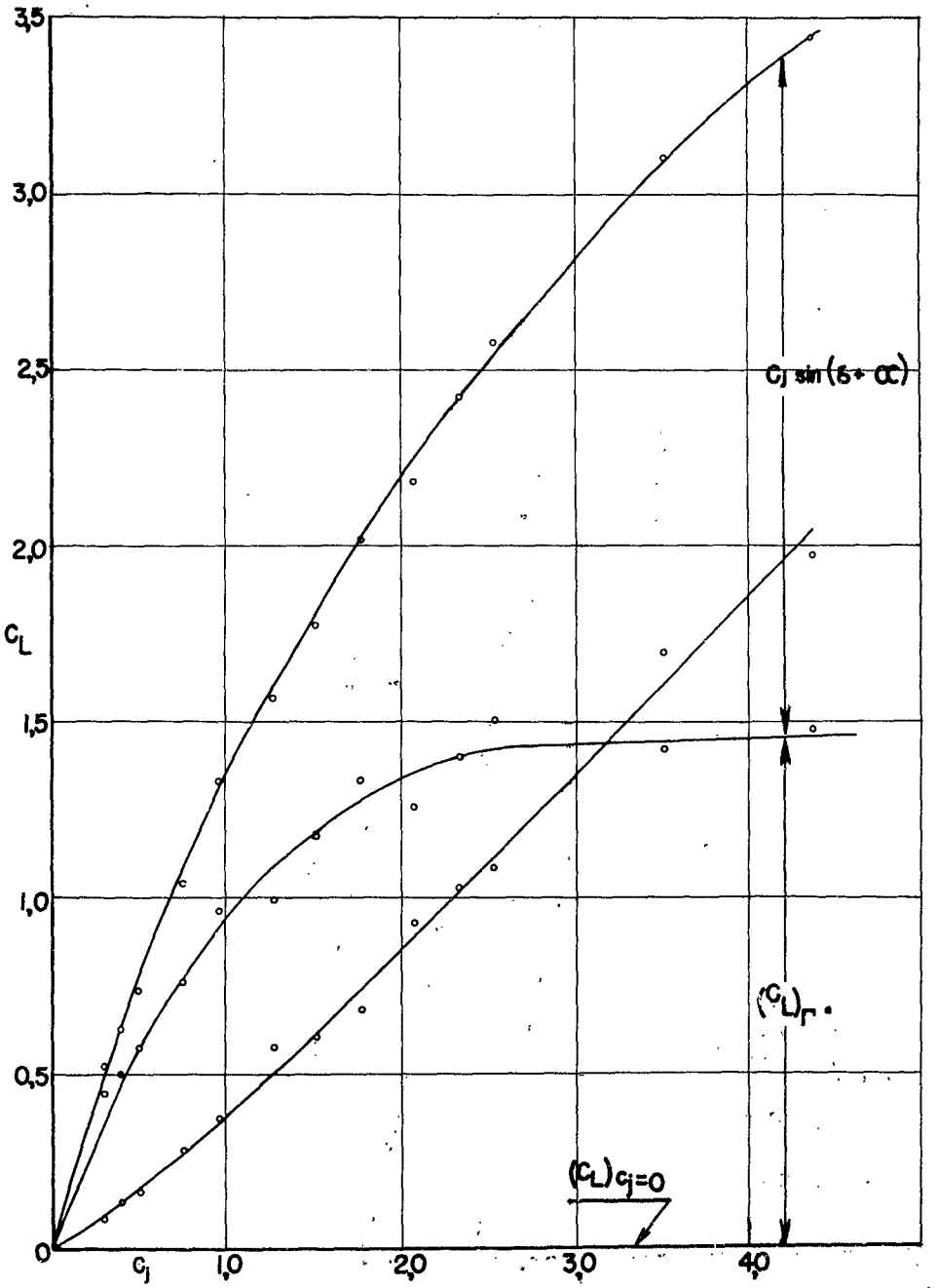

Fig. 22 Variation of lift coefficient with momentum coefficient $\alpha = 0$
Wing with Jet-Flap

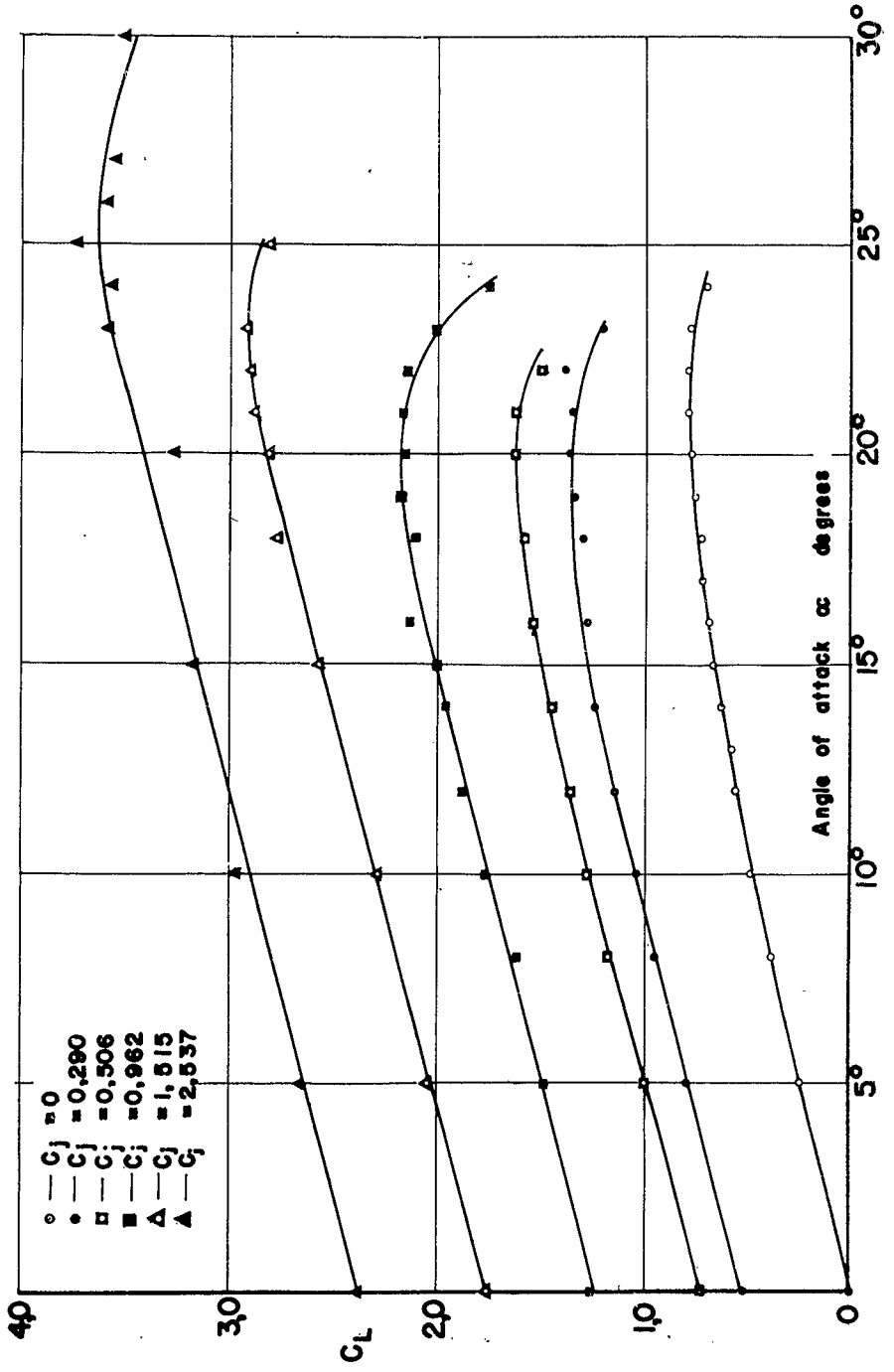

Fig. 23. Variation of lift coefficient with angle of attack with and without jet-flap.

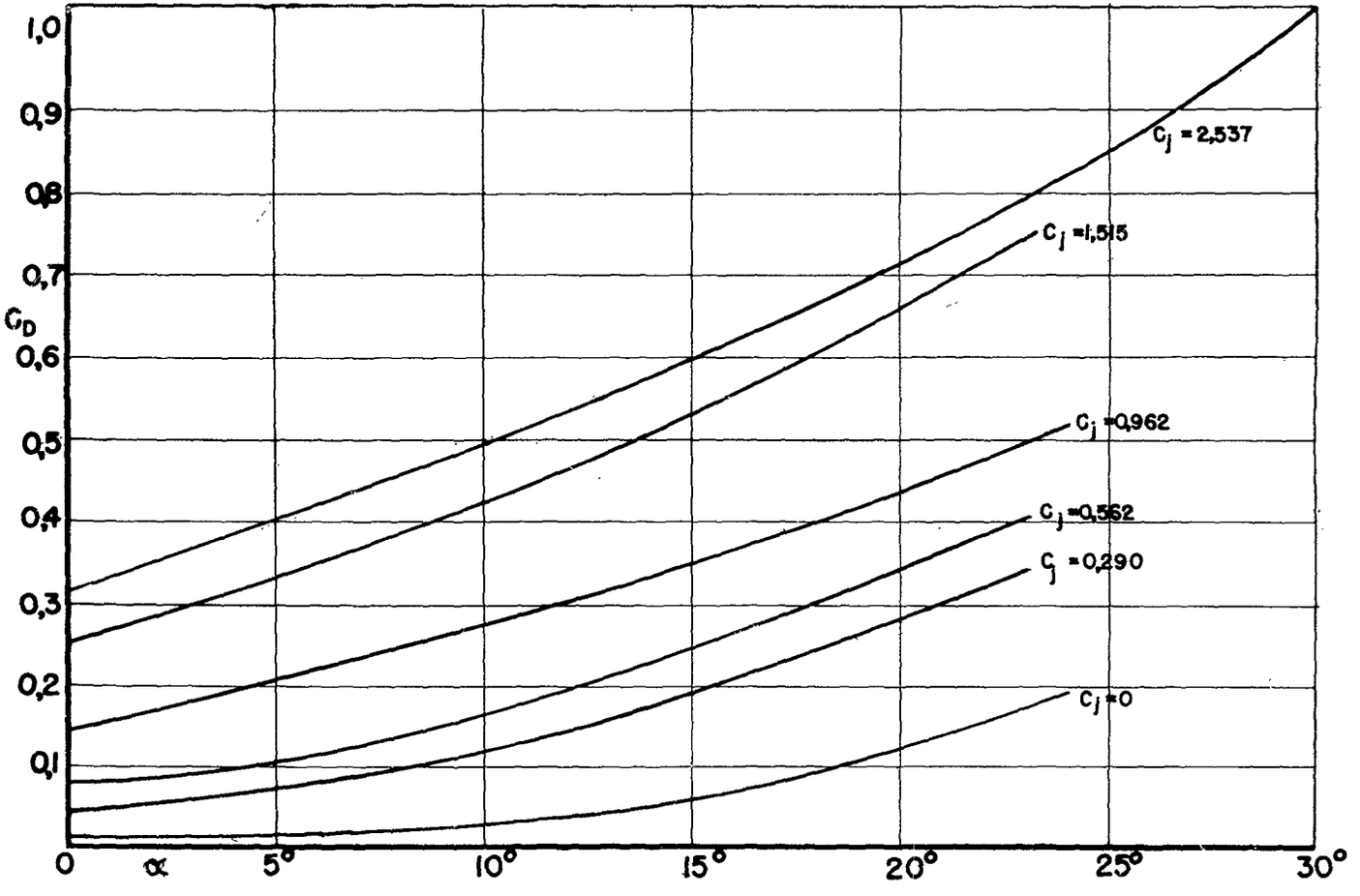

Fig. 24. Variation of drag coefficient with angle of attack with and without jet-flap.

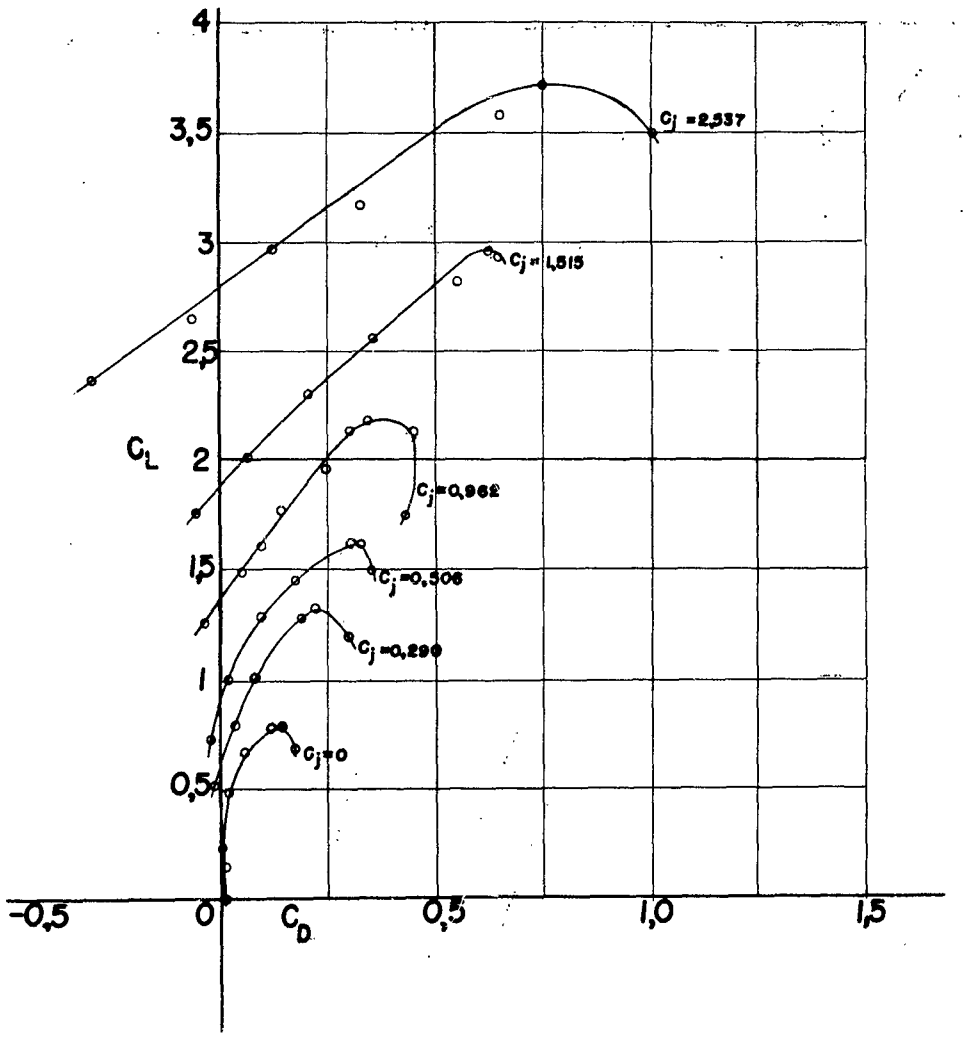

Fig. 25. JET-FLAP – Variation of aerodynamic characteristics with C_j and α $\delta = 60°$

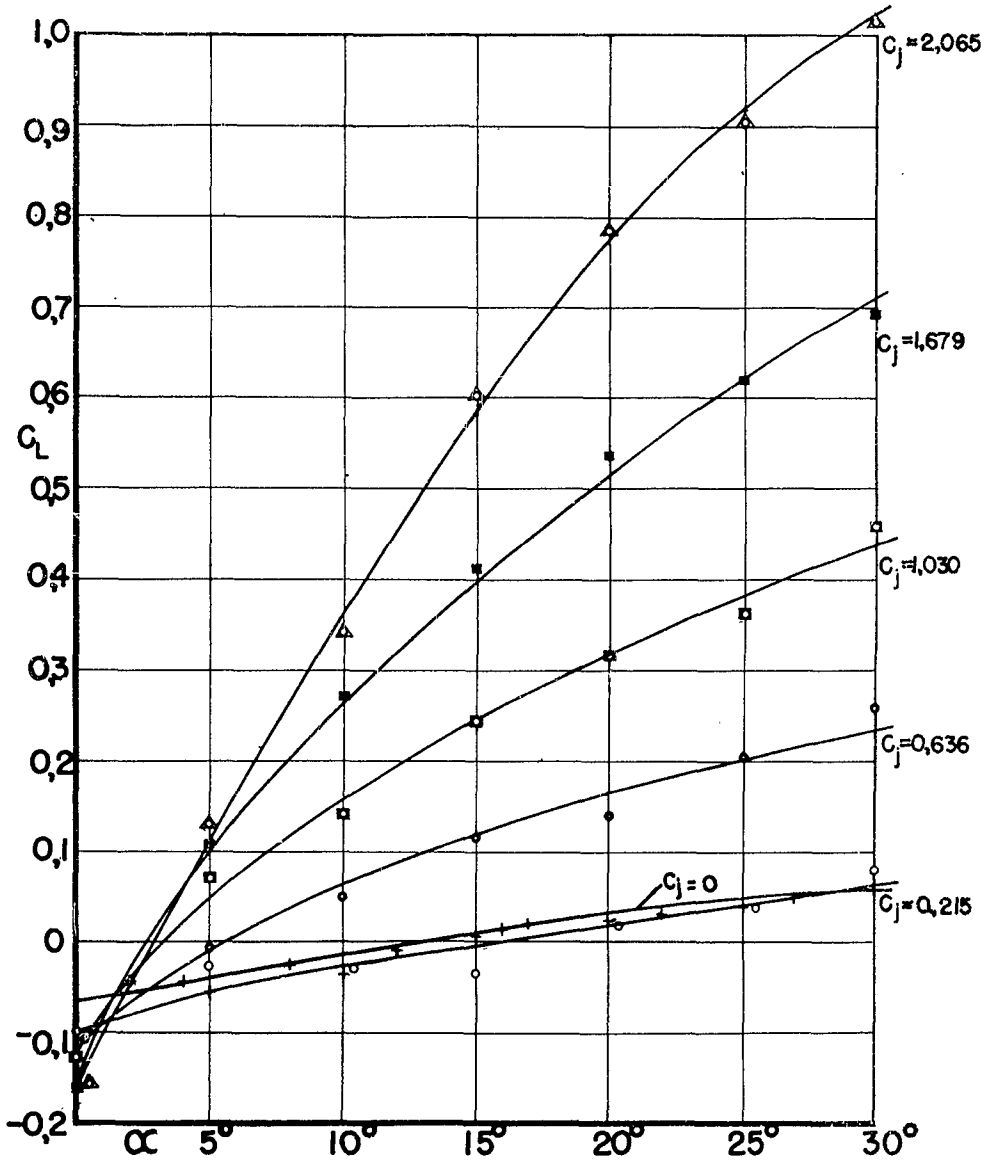

Fig. 26 EXTERNAL JET-FLAP ONLY- Variation of lift coefficient with C_j and α.

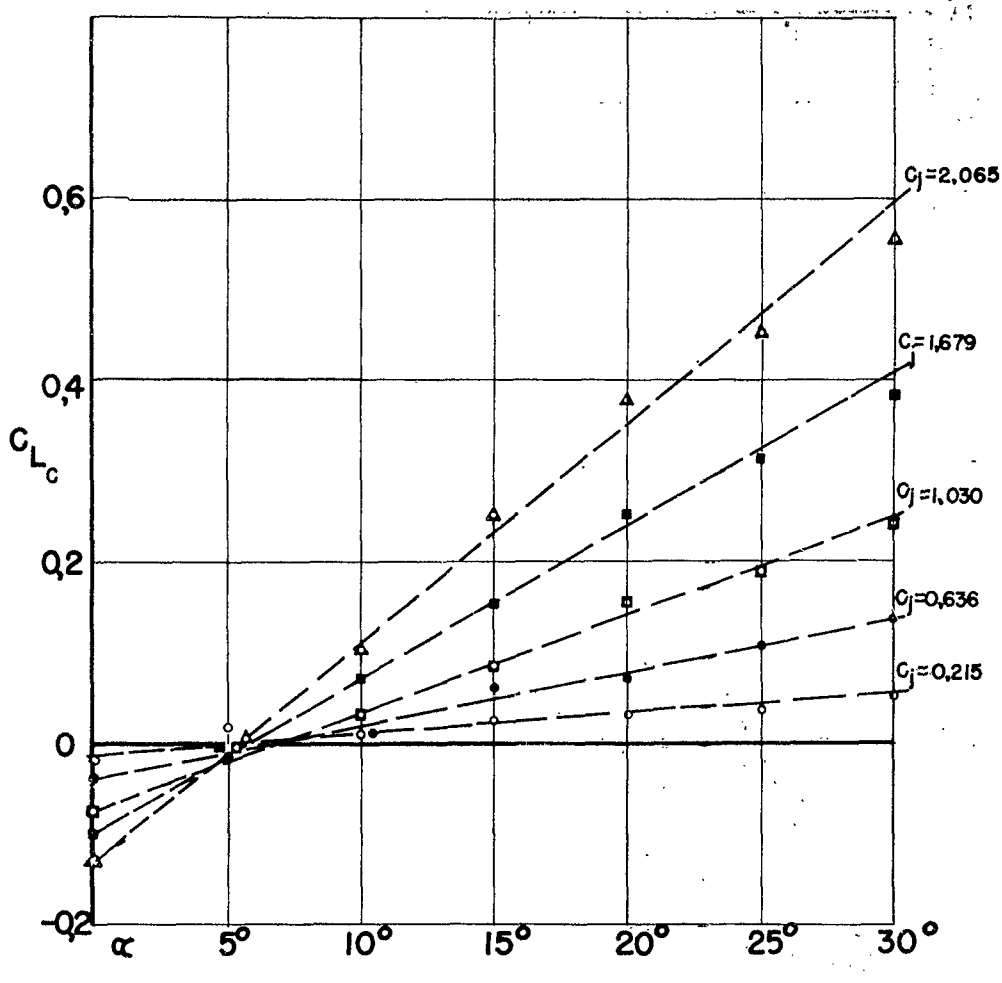

Fig. 27. EXTERNAL JET-FLAP ONLY- Variation of momentum component in lift direction.

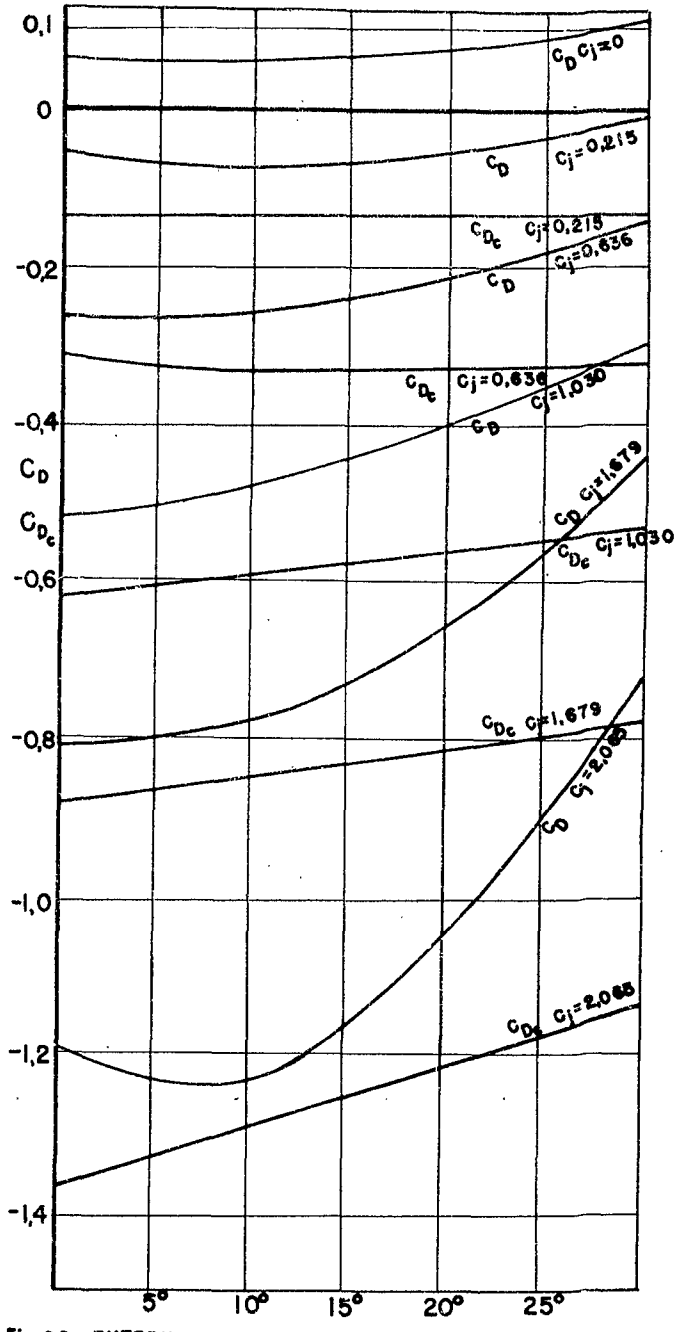

Fig. 28 EXTERNAL JET-FLAP - Variation of total drag and momentum component in drag direction with C_j and α.

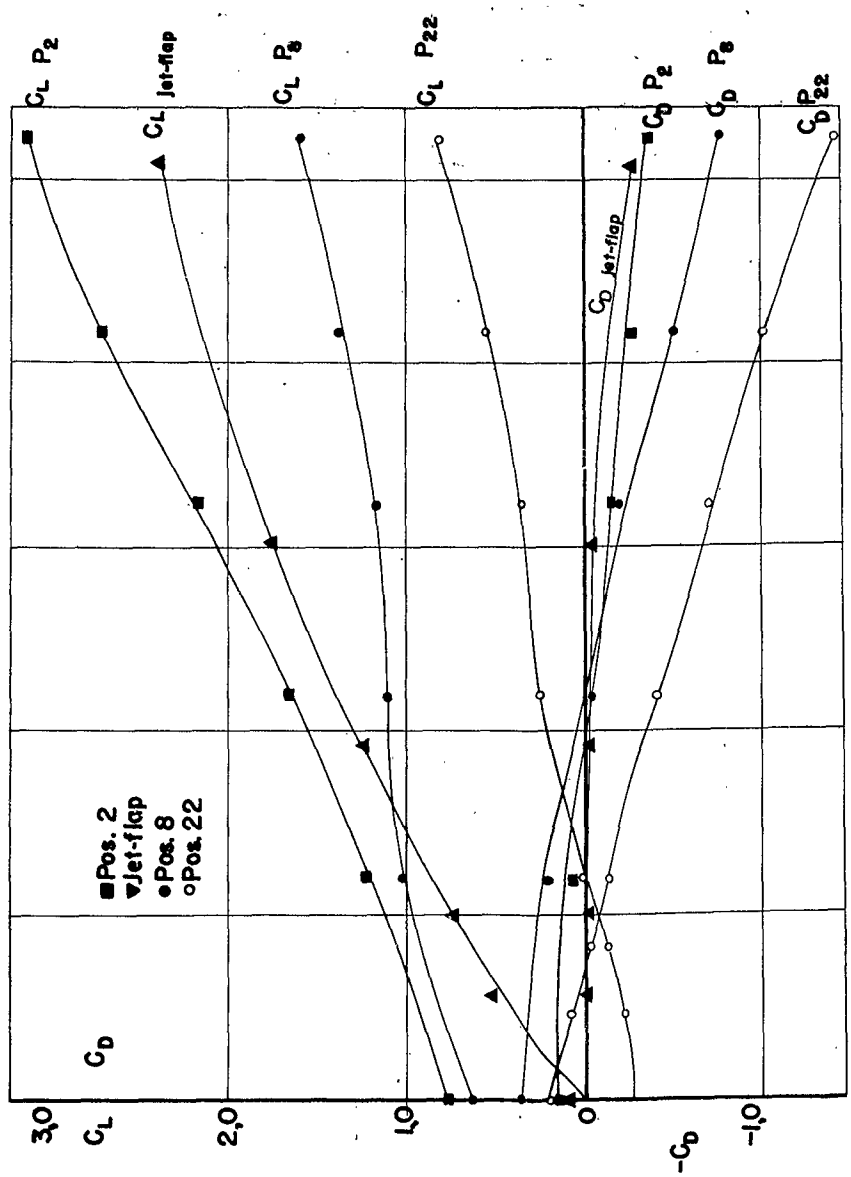

Fig. 29. Comparison of aerodynamic characteristics of the "jet-flap" and external jet-flap in configuration pos. 2, 8 and 22. $\alpha = 0$